The rheumatoid synovial environment alters fatty acid metabolism in human monocytes and enhances CCL20 secretion.

Lewis C. Rodgers[1,2], John Cole[2], Kevin Rattigan[3], Michael P. Barrett[3,4], Nisha Kurian[5], Iain B. McInnes[1], Carl S. Goodyear[1,2*]

[1] Centre of Immunobiology, Institute of Infection, Immunity and Inflammation, College of Medical, Veterinary and Life Sciences, University of Glasgow, Glasgow, United Kingdom

[2] GLAZgo Discovery Centre, Institute of Infection, Immunity and Inflammation, College of Medical, Veterinary and Life Sciences, University of Glasgow, Glasgow, United Kingdom

[3] Wellcome Centre for Molecular Parasitology, Institute of Infection, Immunity and Inflammation, College of Medical, Veterinary and Life Sciences, University of Glasgow, Glasgow, United Kingdom

[4] Glasgow Polyomics, Wolfson Wohl Cancer Research Centre, College of Medical, Veterinary and Life Sciences, University of Glasgow, Glasgow, United Kingdom

[5] Respiratory Inflammation and Autoimmune (RIA) Precision Medicine Unit, Precision Medicine, Oncology R&D, AstraZeneca, Gothenburg, Sweden

* Correspondence to: Prof. Carl S. Goodyear, Sir Graeme Davies Building, 120 University Place, Glasgow, G12 8TA, Scotland, UK. Email: Carl.Goodyear@glasgow.ac.uk

ABSTRACT

Objectives Fatty acid oxidation (FAO) and glycolysis have been implicated in immune regulation and activation of macrophages. However, investigation of human monocytes intracellular metabolism in the context of the hypoxic and inflammatory rheumatoid arthritis (RA) synovium is lacking. We hypothesised that exposure of monocytes to the hypoxic and inflammatory RA environment would have a profound impact on their metabolic state, and potential to contribute to disease pathology.

Methods Human monocytes were isolated from buffy coats and exposed to hypoxia. Metabolic profiling of monocytes was carried out by LC-MS metabolomics. Inflammatory mediator release after LPS or RA-synovial fluid (RA-SF) stimulation was analysed by ELISA. FAO was inhibited by etomoxir or enhanced with exogenous carnitine supplementation. Transcriptomics of RA blood monocytes and RA-SF macrophages was carried out by microarray.

Results Hypoxia exacerbated monocyte-derived CCL20 and IL-1β release in response to LPS, and increased glycolytic intermediates at the expense of carnitines. Modulation of carnitine identified a novel role for FAO in the production of CCL20 in response to LPS. Transcriptional analysis of RA blood monocytes and RA-SF macrophages revealed that fatty acid metabolism was altered and CCL20 increased when monocytes enter the synovial environment. *In vitro* analysis of monocytes showed that RA-SF increases carnitine abundance and CCL20 production in hypoxia, which was exacerbated by exogenous carnitine.

Conclusion This work has revealed a novel inflammatory mechanism in RA that links FAO to CCL20 production in human monocytes, which could subsequently contribute to RA disease pathogenesis by promoting the recruitment of Th17 cells and osteoclastogenesis.

Keywords:

Inflammation, Metabolism, Monocytes, Rheumatoid arthritis, Synovial fluid, Hypoxia, CCL20

Key messages:

1. Hypoxia modifies monocyte metabolism and exacerbates the release of pro-inflammatory mediators.
2. The RA synovial milieu severely alters fatty acid metabolism, which supports the release of CCL20 from monocytes.

INTRODUCTION

Rheumatoid arthritis (RA) is a chronic inflammatory disease characterised by immune-mediated pathology and articular destruction. Enhanced metabolic turnover and a disrupted vasculature creates hypoxic regions (<1% O_2) within the affected synovium in comparison to the normal synovium which can range from 5-8% O_2 (1,2). Such low pO_2 levels in the RA synovium likely contribute to infiltration of leukocyte subsets that in turn drive disease pathogenesis (3). Monocytes and macrophages are considered central to pathogenesis by virtue of their capacity to release inflammatory cytokines, chemokines and reactive oxygen and nitrogen intermediates. They can be activated by various molecules such as immune complexes, TLR agonists, complement factors, T cell cognate interactions and thereby drive chronicity. Infiltrating monocytes, therefore, must undergo substantial metabolic adjustment in this context that likely confers functional impact on their behaviours and contribution to pathology.

Although largely studied in experimental settings, metabolic pathways, such as glycolysis and fatty acid β-oxidation (FAO), are increasingly implicated in the governance of immune-mediated cascades in macrophages. Glycolysis is one of the best characterised metabolic pathways in the immune-metabolic field. In particular, glycolysis is thought to drive the inflammatory phenotype of M(LPS ± IFNγ) macrophages and the production of IL-1β in a process mediated by succinate accumulation and HIF-1α (4,5). FAO is a mitochondrial process whereby fatty acids are converted to products such as acetyl-CoA to generate energy. In order for medium and long-chain fatty acids to enter the mitochondria for oxidation, they are first conjugated to free carnitine by the enzyme, carnitine palmitoyltransferase I (CPT1). This complex is then shuttled through the mitochondrial membrane where fatty acid acyl-

CoA groups are released from carnitine into the mitochondrial matrix by carnitine palmitoyltransferase II (CPT2) for subsequent oxidation (6). FAO was considered essential for the induction of the M(IL-4) murine macrophage metabolic programme (7,8), although this notion has been challenged in the 'equivalent' M(IL-4) macrophage phenotype in humans, where FAO appears to be dispensable (9). There is evidence, however, to suggest that FAO can dampen immune responses in macrophage cell lines in response to palmitate (10). How FAO influences specific functions in human myeloid cells remains poorly understood.

Furthermore, there are only a limited number of studies on immune-metabolism in the context of RA. It has previously been shown that monocytes and macrophages from RA patients express high levels of α-enolase (a glycolytic enzyme) on the cell surface, which can be bound mainly in citrullinated form, by autoantibodies to induce the production of inflammatory cytokines including TNFα and IFNγ (11). More recent studies interrogating macrophages derived from RA patients, defined increases in both mitochondrial and glycolytic metabolism, associated with a hypermetabolic profile (12). Moreover, RA synovial fluid (RA-SF) derived succinate has been shown to signal through GPR91 to promote IL-1β release from murine macrophages (13).

We set out, therefore, to define the impact of key components of the synovial microenvironment on monocyte metabolism using hypoxia and TLR agonists as surrogates, and RA synovial fluid as a definitive stimulus. We report that the production of CCL20 is regulated by the FAO set-point in monocytes, which is heavily influenced by the microenvironment to which they are exposed. Taken together, we have uncovered a key novel pathway that could contribute to disease pathogenesis through the recruitment of pathogenic Th17 cells and the enhancement of osteoblast-mediated osteoclastogenesis (14-16)

METHODS

Detailed information of the following methods are provided in the online supplementary data.

Human samples, patients and controls

Buffy coats from the Scottish National Blood Transfusion Service (SNBTS) from healthy volunteers were used to isolate primary human cells. Synovial fluid was obtained from rheumatoid arthritis (RA) patients, which were identified from Rheumatology clinics at the Glasgow Royal Infirmary and fulfilled the 2010 ACR/EULAR criteria for RA. All samples were obtained after written consent, with the appropriate ethical approvals in place. Patient characteristics for microarray analysis are illustrated in (18). Synovial fluid was obtained from RA patients with active disease that required aspiration of a joint with effusion.

Primary human monocyte isolation and culture

Peripheral blood mononuclear cells (PBMCs) were separated from human blood buffy coats by density gradient centrifugation and monocytes purified using the EasySep monocyte enrichment kit, without CD16 depletion (StemCell Technologies). Human monocytes were stimulated with either 10 ng/ml LPS-EK ultrapure (Invivogen) or 10% RA synovial fluid. For carnitine manipulation, monocytes were treated with 10 mM L-carnitine (Sigma-Aldrich) simultaneously with LPS or RA synovial fluid stimulation. Monocytes were pre-treated for 1 hour with etomoxir (ETO; Sigma-Aldrich) at 50 μM.

Induction of hypoxia

For the induction of hypoxia (1% O_2), an airtight hypoxic chamber was utilised (Billups-Rothenburg). For culture in normoxia (20% O_2), cells were cultured in ambient oxygen in a standard 37°C tissue culture incubator.

Extraction of monocyte intracellular metabolites

Intracellular metabolites were harvested from monocytes by chloroform:methanol:water (1:3:1 ratio) extraction at ≤4°C. Samples were stored in screw-capped vials at -80°C until analysis.

Untargeted Liquid Chromatography Mass Spectrometry (LC-MS)

Hydrophilic interaction liquid chromatography (HILIC) was carried out on a Dionex UltiMate 3000 RSLC system (Thermo Fisher) using a ZIC-pHILIC column (Merck Sequant). For the MS analysis, a Thermo Orbitrap Q Exactive (Thermo Fisher) was operated in both positive and negative mode.

Processing of MS data

Processing of the raw data and analysis was performed using a processing pipeline through IDEOM Excel based software (17). According to the metabolomics standards initiative (MSI), metabolite identifications (MSI level 1) are given when more than one feature matches an authentic standard (i.e. mass and retention time) and annotations are made when matching to a metabolite is made by mass only (MSI level 2), and should be considered putative. Normalised data was used in generating the principal component analysis (PCA) and heatmaps. PCA was performed on the processed metabolite data using the R (v.3.4.4) function prcomp. Heatmaps of significant metabolites were hierarchically clustered using the R package hclust, with the distance method Spearman and cluster method Average. The data was then scaled into per metabolite z-scores (i.e. distance from the mean in units of standard deviations) using the R function scale.

Microarray Analysis

RNA purification and microarray analysis of samples from matched RA blood and SF derived CD14+ cells was conducted as previously described (18). In brief, the raw data (.CEL files) were processed and normalised using R (version 3.4.4). The R WGCNA package was used to collapse multiple genes down to a single value using the “MaxMean” method.

Differential expression was determined using the R package LIMMA (19) with a significance threshold of adjusted $p < 0.05$ and a fold change > 2. Enriched gene-sets were determined using a hypergeometric test with Benjamini-Hochberg correction at $p < 0.05$. The collapsed probe-set was used as the background, and a combination of the following MsigDB (20) collections were used in the analysis: canonical pathways, BIOCARTA, KEGG, REACTOME and GO.

ELISA & Meso-Scale Discovery (MSD)

Supernatant analysis of IL-1β (Life Technologies) and CCL20 (R&D Systems) was carried out by ELISA according to the manufacturer's instructions.

TNFα, IL-1β and IL-6 supernatant were also analysed by using the V-PLEX Pro-inflammatory panel 1 from MSD according to the manufacturer's protocol.

Statistical Analysis

Statistical analysis was performed in GraphPad Prism 6 software. All data are shown as the mean ± standard deviation (SD) unless otherwise stated. The statistical test used for each experiment is indicated in the figure legend. A *p* value of less than 0.05 was considered significant.

Data Availability

The microarray array data is MIAME compliant and has been deposited to the ArrayExpress database (http://www.ebi.ac.uk/arrayexpress) with the accession number: E-MEXP-3890. Metabolomic data will be deposited to the MetaboLights database (https://www.ebi.ac.uk/metabolights).

RESULTS

Hypoxia enhances the release of pro-inflammatory mediators from LPS stimulated human monocytes

We initially set out to confirm that hypoxia, as observed in the synovial microenvironment, would potentiate the ability of human monocytes to secrete pro-inflammatory mediators (21). Human monocytes from healthy individuals were exposed to hypoxic conditions and stabilisation of HIF-1α was verified (Figure 1A). We analysed the secretion of IL-1β, IL-6, TNFα and CCL20 in both resting and LPS-activated monocytes exposed to hypoxia for 16 hours. CCL20 was included, as it had previously been reported to be a hypoxia-inducible chemokine in human monocytes (22). Unstimulated monocytes did not spontaneously secrete any of the evaluated cytokines or chemokines when cultured in normoxia (Figure 1B). Moreover, hypoxia alone did not induce release of IL-1β, IL-6, TNFα or CCL20 (Figure 1B). LPS induced secretion of IL-1β, IL-6, TNFα and CCL20 in monocytes in normoxia, and this was significantly increased by hypoxia (Figure 1B). Notably, there was a four-fold increase in the release of CCL20 in hypoxic conditions compared to normoxia ($p = 0.001$). With regards to TNF secretion, this was a donor-specific phenomenon (Figure 1B). These data suggest that upon adaptation to a hypoxic inflammatory environment, monocytes are primed to enhance their ability to secrete pro-inflammatory mediators.

Short-term hypoxia reduces carnitine abundance in human monocytes

We postulated that hypoxia-specific metabolic reprogramming was priming monocytes to augment their ability to secrete inflammatory cytokine/chemokines in response to LPS. Using the same hypoxic culture system, we first examined how monocytes metabolically adapted to low pO_2 by conducting LC-MS based metabolomics. PCA analysis revealed that monocytes exposed to hypoxia exhibited a distinct metabolic profile to those cultured in normoxia

(Figure 2A). Monocytes exposed to hypoxia had 23 significantly altered metabolites. Thirteen of these metabolites were of higher abundance in hypoxic conditions, while 10 metabolites were of lower abundance (Figure 2B & Supplementary Table 1). This corresponded to increased glycolytic and purine intermediates and decreased mitochondrial-associated metabolites (Supplementary Table 1). Further interrogation of the mitochondrial-associated metabolites revealed that one of the most prominent reductions was in the acylcarnitine, O-propanoylcarnitine (Figure 2C). Interestingly, we also observed donor specific decreases in free carnitine (L-carnitine) and another acylcarnitine, 2-methylbutyroylcarnitine (Figure 2C). This suggested that carnitine shuttling (Figure 2D) is altered during the adaptation process to hypoxia, and that this change could have a subsequent negative impact on downstream FAO. In contrast to carnitine metabolites, a reverse effect was observed in glycolytic-associated metabolites. Notably, of the 8 glycolytic metabolites that were putatively identified, 4 were significantly up-regulated after 4 hours of hypoxia. We observed an increase in the glycolytic intermediates 3-P-glycerate, fructose-1-6-bisphosphate glyceraldehyde-3-P and D-glucose (Figure 2E). This was associated with a significant increase in the transcript level of the glycolytic enzymes *GLUT-1*, *HK2, PGK1* and *LDHA* (Supplementary Figure S1). Evaluation of intermediates involved in purine metabolism revealed that select metabolites (IMP and hypoxanthine) were also increased in hypoxic conditions (Supplementary Figure S2). Together, these data suggest that glycolytic metabolism is increased at the expense of carnitine-dependent FAO for ATP production during monocyte adaptation to hypoxia.

Carnitine modulation implicates a role for FAO in the production of pro-inflammatory mediators

We next tested the notion that the balance between glycolysis and carnitine shuttling (and subsequent FAO) provides a functional link to the enhanced secretion of inflammatory

mediators up on adjustment to hypoxic conditions. We pharmacologically blocked carnitine-dependent FAO. Pre-treatment with etomoxir (ETO, a carnitine palmitoyltransferase I [CPT1] inhibitor) significantly increased the level of IL-1β secretion in LPS stimulated cells, in both normoxia and hypoxia (Figure 3A). This suggests that ETO shifts cellular metabolism towards increased glycolysis, which in turn exacerbates IL-1β production (4). In contrast, although ETO significantly increased the production of CCL20 from monocytes in response to LPS ($p = 0.03$) it had no effect on the production of CCL20 in hypoxic conditions (Figure 3A). We therefore concluded that in normoxic conditions, enhanced glycolysis (via ETO) exacerbates CCL20 production. In hypoxia, however, the balance between glycolysis and FAO metabolism is such that ETO cannot shift it further and hence there is no increase in glycolysis-driven CCL20 production.

To further investigate the role of these metabolic pathways on cytokine/chemokine release, human monocytes (from a distinct donor cohort to the ETO experiments) were cultured in the presence of exogenous carnitine (10 mM) to enhance FAO. This concentration was utilised as it did not impair monocyte viability (Supplementary Figure S3). Exogenous carnitine had no significant impact on the production of IL-1β (Figure 3B). Surprisingly, exogenous carnitine significantly enhanced the production of CCL20 from LPS-stimulated monocytes in both normoxic and hypoxic ($p = 0.0156$) conditions (Figure 3B). Together these data suggest that both glycolysis and FAO can contribute to the production of CCL20 in human monocytes. The precise weighting of these pathways in driving CCL20 production in chronic disease may be dependent on the metabolic phenotype induced by specific stimuli and environmental factors in the disease state.

Monocyte adaptation to the RA synovial compartment induces transcriptional alterations in CCL20 & fatty acid metabolic pathways.

To investigate if CCL20 and fatty acid metabolism were altered when human monocytes adapted to the hypoxic and inflammatory RA synovial environment *in vivo*, we re-analysed microarray data that compared circulating blood monocytes with matched synovial fluid macrophages from RA patients (18). Using a 2-fold cut-off and an adjusted *p* value of 0.05, we identified 2217 differentially expressed genes (Figure 4A). Consistent with our *in vitro* data (Figure 1B), CCL20 was significantly increased in RA-SF macrophages (Figure 4B). To identify additional pathways that were significantly altered between RA-SF macrophages and blood monocytes, we conducted hypergeometric pathway analysis. Interestingly, this analysis identified 5 pathways associated with fatty acid metabolism (i.e., FAO and transport) that were significantly altered (Figure 4C and Supplementary Figure S4).

RA-SF increases the abundance of carnitine metabolites in monocytes, which can support CCL20 release.

To interrogate the relevance of these transcriptional changes, we investigated whether carnitine-mediated FAO was modified by a surrogate for synovial conditions *in vitro*. To replicate the synovial microenvironment, we cultured monocytes under hypoxic conditions and stimulated the cells with media containing RA-SF. The monocyte metabolic profile was analysed by LC-MS and LPS was utilised as a comparator stimulus. PCA analysis demonstrated that monocytes exposed to hypoxia and RA-SF have subtle differences in metabolome compared to those cultured in hypoxia with or without LPS (Figure 5A). Subsequent analysis revealed that stimulation of monocytes with RA-SF in hypoxic conditions significantly increased ($p < 0.05$) 33 metabolites in comparison to both hypoxia-exposed or LPS stimulated hypoxia-exposed monocytes (Figure 5B & Supplementary Table 2). In particular, analysis at a single metabolite level revealed that L-carnitine and the acyl-carnitines; 3-dehydroxycarnitine and O-acetylcarnitine, were significantly increased in human monocytes by RA-SF in hypoxia. (Figure 5B and 5C). In addition, metabolic

intermediates of purine breakdown (xanthine and urate; Figure 5B and Supplementary Figure S6) and creatinine biosynthesis (Supplementary Figure S5) were altered by RA-SF. Furthermore, we observed increases in intracellular ATP upon RA-SF treatment (Supplementary Figure S7).

Taking the microarray and *in vitro* metabolomic analyses together, we hypothesised that carnitine shuttling (and potentially FAO) affects cytokine and chemokine secretion (in particular, CCL20) in the context of disease-specific (RA-SF) stimulation of human monocytes. Therefore, this pathway was inhibited or increased via ETO or exogenous carnitine treatment respectively. In contrast to LPS stimulation, RA-SF did not induce detectable levels of IL-1β (data not shown). However, RA-SF stimulation was able to induce CCL20 secretion, the magnitude of which was donor specific (Figures 6A & 6B). Pre-treatment with ETO had no observable effect on CCL20 release (Figure 6A). In contrast, the addition of exogenous carnitine significantly enhanced the release of CCL20 in hypoxic conditions (Figure 6B). Interestingly, in a proportion of donors where no detectable levels of CCL20 were observed in hypoxia, treatment with RA-SF resulted in detectable levels of CCL20. These results indicate that carnitine shuttling and subsequent FAO potentially has an important role in the production of CCL20 under hypoxic conditions in response to disease-specific stimuli.

DISCUSSION

The RA synovial compartment is a complex milieu that contains both stimulating factors and hypoxic regions. However, these environmental exposures are not routinely taken into consideration in immune-metabolic studies. We have demonstrated that the RA synovial environment has profound and distinct effects on the metabolic profile of human monocytes, particularly in fatty acid metabolism. This leads to resetting of the balance between FAO and

glycolysis that can determine the levels of CCL20 and IL-1β production. Furthermore, by manipulating carnitine levels *in vitro*, our studies reveal that FAO has an important role in the production of CCL20 in both LPS and RA-SF stimulated cells suggesting increased carnitine abundance, potentially as part of a hypermetabolic state (12), can drive a CCL20-mediated inflammatory cascade to promote disease pathogenesis.

Our studies confirmed that hypoxia increases glycolytic metabolism at the expense of mitochondrial pathways, such as carnitine-dependent FAO, in human monocytes (23,24). Increased glycolytic flux is commonly associated with inflammatory macrophages suggesting that hypoxia induces a metabolic switch to promote an inflammatory phenotype (4,25). Indeed, in response to LPS challenge, hypoxia substantially increased the production of the pro-inflammatory cytokines IL-6 and IL-1β, from monocytes. In addition, hypoxia also exacerbated CCL20 production, which is consistent with the notion that CCL20 is a hypoxia-associated factor (21). These data align with a recent study in human macrophages, where hypoxia increased the release of IL-6 and IL-1β in response to palmitate (22). Together, this suggests that hypoxia acts as an extracellular danger signal that primes a robust inflammatory response through transcriptional and metabolic rewiring.

FAO has been proposed to govern the polarisation of M(IL-4) murine macrophage (7). In contrast, recent studies have concluded that FAO has a dispensable role in M(IL-4) polarisation in human macrophages (9,26). Leaving us to question what roles FAO may have on immune-mediated mechanisms in human myeloid cells. In order to determine if carnitine and subsequent FAO plays a role in the exacerbated release of pro-inflammatory mediators, carnitine shuttling was targeted for inhibition via ETO or enhanced by supplementation with exogenous carnitines. We found that enhancing cellular carnitine through exogenous supplements significantly elevated CCL20 release. In addition, exogenous carnitine had donor specific effects on IL-1β. Therefore, the precise role of FAO on IL-1β production

warrants further investigation in a larger study. This is however in contrast to previously published work, which suggested that carnitine supplementation was immunosuppressive and attenuated the release of IL-1β, IL-6 and TNFα from murine macrophages (27). In this instance, suppression was observed with 100 mM of L-carnitine treatment. In our experimental conditions however, concentrations greater than 10 mM negatively affected primary human monocyte viability (Supplementary Figure S3). These data suggest that primary human monocytes and murine macrophages have differing sensitivity to, and functional consequences upon, exposure to exogenous carnitine. In comparison, carnitine shuttling inhibition via ETO substantially increased IL-1β in both oxygen tensions. Treatment of prostate cancer cells with ETO has previously been shown to decrease lipid oxidation and augment the uptake of glucose, expression of hexokinase-2 and the release of lactate from these cells (28). Therefore, the increase in IL-1β under these circumstances could be attributed to increased glycolytic flux. Indeed, in M(LPS + IFNγ) macrophages, glycolysis is thought to drive increased IL-1β production (4), implying that monocytes and macrophages both require glycolytic metabolism to promote IL-1β production.

Our transcriptomic interrogation demonstrated that fatty acid metabolic pathways are severely altered when monocytes infiltrate from the blood and adapt to the RA synovium. In support of this concept, *in vitro* metabolomic analyses revealed increased abundance of carnitine and its acyl derivatives, and potentially FAO in RA-SF treated monocytes. Recently studies revealed that $CD14^+$ monocytes and *in vitro* generated macrophages from RA patients with active disease also increased mitochondrial metabolism by increasing oxygen consumption (12). Interestingly, macrophages from RA patients also exhibit increased glycolysis and ATP that suggest RA-associated macrophage are hypermetabolic (12). However, in our study RA-SF did not induce any significant alterations in the 3 glycolytic intermediates (D-glucose; D-glyceraldehyde-3-P and pyruvate), which were putatively

identified in our untargeted MS dataset. Nonetheless, in support of the study, we did observe increases in ATP production in monocytes stimulated in RA-SF (Supplementary Figure S7).

In addition to the altered fatty acid pathways, our microarray analysis illustrated that CCL20 was significantly increased upon monocyte adjustment to the RA synovial compartment. Therefore, we postulated that the levels of carnitine-mediated FAO could influence the release of CCL20 under RA synovial conditions *in vitro*. In a finding shared with LPS stimulated cells, exogenous carnitine exacerbated CCL20 production from human monocytes in response to RA-SF in hypoxic conditions. This suggests that intracellular carnitine and subsequent FAO promotes CCL20 release in response to cascades induced by a number of stimuli that may be present in the RA milieu. The precise signalling events induced by RA-SF remain elusive and may be heterogeneous amongst patients. Interestingly, in LPS treated cells, inhibition of FAO with ETO increased CCL20 only in normoxia. This suggests that in hypoxia there was saturated CCL20 release under these conditions. Taken together, our carnitine modulation experiments indicate that both FAO and glycolysis could act in conjunction to promote CCL20 production. Specifically, these data point to a novel inflammatory link between FAO and the production of CCL20. We speculate that increased abundance of acylcarnitines and thus, acyl-donors, through carnitine shuttling may increase protein acylation to regulate CCL20 production. In support of this, exacerbation of FAO can increase the mitochondrial pool of acetyl-CoA, which act as donors for histone acetyltransferases (HATs) for the addition of acetyl groups to lysine residues on target proteins (29). Indeed, the transcriptional coactivators, CREB-binding protein and p300, which have known HAT-activity, have been reported to bind the CCL20 promoter and increase gene expression in activated astrocytes and pancreatic β-cells (30,31). Direct acylation through acylcarnitine donors could also occur, although little is known about such reactions involving acylcarnitines.

Further work is, however, required to identify the exact mechanism for FAO-mediated CCL20 release in monocytes. This is important, as CCL20 is being increasingly implicated in inflammatory cascades in RA. For example, it has been reported to be secreted by IL-1β stimulated fibroblast-like synoviocytes, and can in turn promote chemotaxis of pathogenic $CCR6^+$ Th17 cells (32). Moreover, recent studies have shown that CCL20 can induce the migration of B cells purified from RA peripheral blood (33). Combined this supports a role for infiltrating monocyte-derived CCL20 in promoting pathogenic $CCR6^+$ Th17 and B cell accumulation in the RA synovial compartment. A role for CCL20 in osteoblast-mediated osteoclast differentiation and subsequent resorption activity in the synovial compartment has also been identified (15). This suggests that in addition to promoting adaptive immune cell infiltration, CCL20 can enhance bone erosion in the RA joint.

Overall, this report has elucidated a novel mechanism that links fatty acid metabolism to the release of CCL20 from human monocytes in the RA milieu. We propose that upon infiltration into the RA synovial environment, monocytes alter their fatty acid metabolic machinery that in turn can support CCL20-mediated inflammation in RA (Supplementary Figure S8). Our data provide additional supportive evidence that intracellular metabolism can govern immunological pathways in chronic inflammatory diseases.

REFERENCES

1. Lund-Olesen K. Oxygen tension in synovial fluids. Arthritis & Rheumatism. 1970;13:769–76.

2. Fearon U, Canavan M, Biniecka M, Veale DJ. Hypoxia, mitochondrial dysfunction and synovial invasiveness in rheumatoid arthritis. Nat Rev Rheumatol. 2016;12:385–97.

3. Ng CT, Biniecka M, Kennedy A, McCormick J, Fitzgerald O, Bresnihan B, et al. Synovial tissue hypoxia and inflammation in vivo. Ann Rheum Dis. 2010;69:1389–95.

4. Tannahill GM, Curtis AM, Adamik J, Palsson-McDermott EM, McGettrick AF, Goel G, et al. Succinate is a danger signal that induces IL-1β via HIF-1α. Nature. 2013;496:238–42.

5. Jha AK, Huang SC-C, Sergushichev A, Lampropoulou V, Ivanova Y, Loginicheva E, et al.Network Integration of Parallel Metabolic and Transcriptional Data Reveals Metabolic Modules that Regulate Macrophage Polarization. Immunity. 2015;42:419–30.

6. O'Neill LAJ, Kishton RJ, Rathmell J. A guide to immunometabolism for immunologists. Nat Rev Immunol. 2016;16: 553–65.

7. Huang SC-C, Everts B, Ivanova Y, O'Sullivan D, Nascimento M, Smith AM, et al. Cell-intrinsic lysosomal lipolysis is essential for alternative activation of macrophages. Nat Immunol. 2014;15:846–55.

8. Vats D, Mukundan L, Odegaard JI, Zhang L, Smith KL, Morel CR, et al. Oxidative metabolism and PGC-1beta attenuate macrophage-mediated inflammation. Cell Metab. 2006;4:13–24.

9. Namgaladze D, Brüne B. Fatty acid oxidation is dispensable for human macrophage IL-4-induced polarization. Biochim Biophys Acta. 2014;1841:1329–35.

10. Malandrino MI, Fucho R, Weber M, Calderon-Dominguez M, Mir JF, Valcarcel L, et al. Enhanced fatty acid oxidation in adipocytes and macrophages reduces lipid-induced

triglyceride accumulation and inflammation. Am J Physiol Endocrinol Metab. 2015;308:756–69.

11. Bae S, Kim H, Lee N, Won C, Kim H-R, Hwang Y-I, et al. alpha-Enolase expressed on the surfaces of monocytes and macrophages induces robust synovial inflammation in rheumatoid arthritis. The Journal of Immunology. 2012;189:365–72.

12. Zeisbrich M, Yanes RE, Zhang H, Watanabe R, Li Y, Brosig L, et al. Hypermetabolic macrophages in rheumatoid arthritis and coronary artery disease due to glycogen synthase kinase 3b inactivation. Ann Rheum Dis. 2018;77:1053-62.

13. Littlewood-Evans A, Sarret S, Apfel V, Loesle P, Dawson J, Zhang J, et al. GPR91 senses extracellular succinate released from inflammatory macrophages and exacerbates rheumatoid arthritis. J Exp Med. 2016;213:1655–62.

14. Kaneko S, Kondo Y, Yokosawa M, Furuyama K, Segawa S, Tsuboi H, et al. The RORγt-CCR6-CCL20 axis augments Th17 cells invasion into the synovia of rheumatoid arthritis patients. Mod Rheumatol. 2018;28:814–25.

15. Pathak JL, Bakker AD, Verschueren P, Lems WF, Luyten FP, Klein-Nulend J, et al. CXCL8 and CCL20 Enhance Osteoclastogenesis via Modulation of Cytokine Production by Human Primary Osteoblasts. PLoS ONE. 2015;10:e0131041.

16. Lee AYS, Körner H. CCR6 and CCL20: emerging players in the pathogenesis of rheumatoid arthritis. Immunol Cell Biol. 2014;92:354–8.

17. Creek DJ, Jankevics A, Burgess KEV, Breitling R, Barrett MP. IDEOM: an Excel interface for analysis of LC-MS-based metabolomics data. Bioinformatics. 2012;28:1048–9.

18. Asquith DL, Ballantine LE, Nijjar JS, Makdasy MK, Patel S, Wright PB, et al. The liver X receptor pathway is highly upregulated in rheumatoid arthritis synovial macrophages and potentiates TLR-driven cytokine release. Ann Rheum Dis. 2013;72:2024–31.

19. Ritchie ME, Phipson B, Wu D, Hu Y, Law CW, Shi W, et al. limma powers differential expression analyses for RNA-sequencing and microarray studies. Nucleic Acids Res. 2015;43:47–7.

20. Liberzon A, Subramanian A, Pinchback R, Thorvaldsdóttir H, Tamayo P, Mesirov JP. Molecular signatures database (MSigDB) 3.0. Bioinformatics. 2011;27:1739–40.

21. Bosco MC, Puppo M, Santangelo C, Anfosso L, Pfeffer U, Fardin P, et al. Hypoxia Modifies the Transcriptome of Primary Human Monocytes: Modulation of Novel Immune-Related Genes and Identification Of CC-Chemokine Ligand 20 as a New Hypoxia-Inducible Gene. The Journal of Immunology. 2006;177:1941–55.

22. Snodgrass RG, Boß M, Zezina E, Weigert A, Dehne N, Fleming I, et al. Hypoxia Potentiates Palmitate-induced Pro-inflammatory Activation of Primary Human Macrophages. J Biol Chem. 2016;291:413–24.

23. Huang D, Li T, Li X, Zhang L, Sun L, He X, et al. HIF-1-mediated suppression of acyl-CoA dehydrogenases and fatty acid oxidation is critical for cancer progression. Cell Rep. 2014;8:1930–42.

24. Cramer T, Yamanishi Y, Clausen BE, Forster I, Pawlinski R, Mackman N, et al. HIF-1alpha is essential for myeloid cell-mediated inflammation. Cell. 2003;112:645–57.

25. Rodriguez-Prados JC, Traves PG, Cuenca J, Rico D, Aragones J, Martin-Sanz P, et al. Substrate Fate in Activated Macrophages: A Comparison between Innate, Classic, and Alternative Activation. The Journal of Immunology. 2010;185:605–14.

26. Nomura M, Liu J, Rovira II, Gonzalez-Hurtado E, Lee J, Wolfgang MJ, et al. Fatty acid oxidation in macrophage polarization. Nat Immunol. 2016;17:216–7.

27. Fortin G, Yurchenko K, Collette C, Rubio M, Villani A-C, Bitton A, et al. L-carnitine, a diet component and organic cation transporter OCTN ligand, displays immunosuppressive properties and abrogates intestinal inflammation. Clin Exp Immunol. 2009;156:161–71.

28. Schlaepfer IR, Glodé LM, Hitz CA, Pac CT, Boyle KE, Maroni P, et al. Inhibition of Lipid Oxidation Increases Glucose Metabolism and Enhances 2-Deoxy-2-[18F]Fluoro-d-Glucose Uptake in Prostate Cancer Mouse Xenografts. Molecular Imaging and Biology. 2015;17:529–38.

29. Shakespear MR, Iyer A, Cheng CY, Gupta Das K, Singhal A, Fairlie DP, et al. Lysine Deacetylases and Regulated Glycolysis in Macrophages. Trends Immunol. 2018;39:473–88.

30. Meares GP, Ma X, Qin H, Benveniste EN. Regulation of CCL20 expression in astrocytes by IL-6 and IL-17. Glia. 2012;60:771–81.

31. Burke SJ, Karlstad MD, Regal KM, Sparer TE, Lu D, Elks CM, et al. CCL20 is elevated during obesity and differentially regulated by NF-κB subunits in pancreatic β-cells. Biochim Biophys Acta. 2015;1849:637–52.

32. Tanida S, Yoshitomi H, Nishitani K, Ishikawa M, Kitaori T, Ito H, et al. CCL20 produced in the cytokine network of rheumatoid arthritis recruits CCR6+ mononuclear cells and enhances the production of IL-6. Cytokine. 2009;47:112–8.

33. Armas-González E, Domínguez-Luis MJ, Díaz-Martín A, Arce-Franco M, Castro-Hernández J, Danelon G, et al. Role of CXCL13 and CCL20 in the recruitment of B cells to inflammatory foci in chronic arthritis. Arthritis Res Therapy. 2018;17:1–12.

Funding

This work was supported by AstraZeneca (GLAZgo Discovery Centre)

Competing Interests.

NK is an employee of AstraZeneca. IBM and CSG have received consultancies and grants from AstraZeneca. The other authors declare no competing financial interests.

Acknowledgements.

We would like to thank Erin Manson, Ana Monteiro and Suzanne McGill (Glasgow Polyomics, University of Glasgow) for their assistance with LC-MS experiments.

Author Contributions.

Conceived and designed the experiments: LCR, MPB, NK, IBM, CSG. Performed the experiments: LCR, KR. Analysed the data: LCR, JC, CSG.; wrote manuscript: LR, NK, IBM, CSG

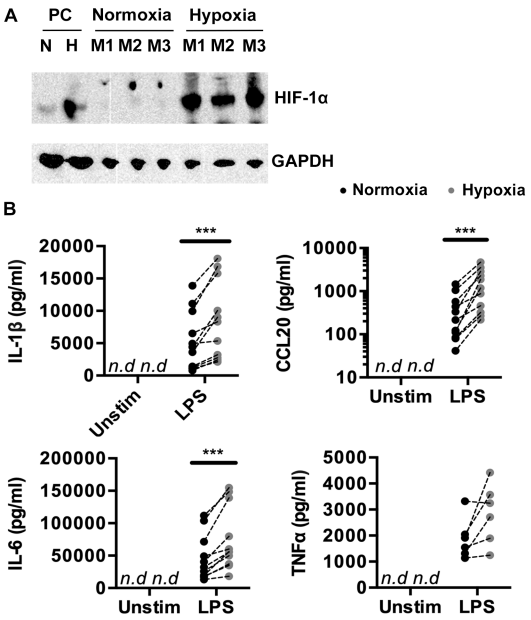

Figure 1. Hypoxia exacerbates the release of pro-inflammatory mediators from LPS stimulated monocytes. [A] Monocytes cultured for 4h in normoxia (20% O_2) or hypoxia (1% O_2) and immunoblotted for HIF-1α and GAPDH (loading control). Positive control (PC) HeLa cell lysate cultured in normoxia (N) or hypoxia (H) was also probed. $N = 3$ **[B]** Monocytes cultured in normoxia or hypoxia ± LPS (10 ng/ml) for 16h. Cell-free supernatant was harvested and assessed by MSD (IL-6, IL-1β & TNFα) and ELISA (CCL20). Statistically analysed by paired *t* Test (IL-6 & IL-1β) or Wilcoxon rank test (CCL20 & TNFα) after D'Agostino & Pearson normality testing. $N = 6\text{-}11$. *** $p \leq 0.001$. *n.d.* = non-detectable.

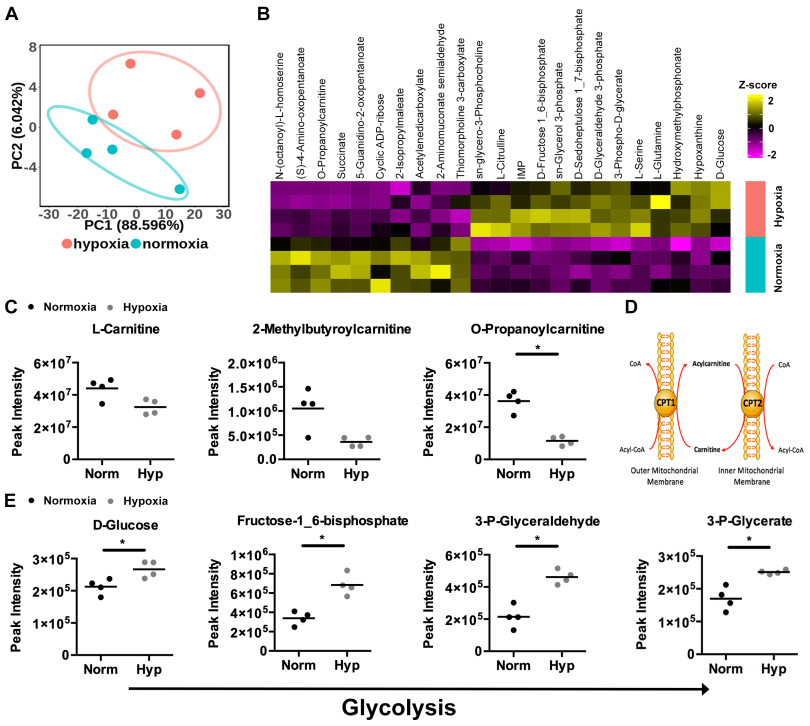

Figure 2. Hypoxia alters the metabolome of human monocytes. Monocytes cultured for 4h in normoxia (20% O_2) or hypoxia (1% O_2) and intracellular metabolites analysed by LC-MS. **[A]** PCA analysis of metabolic profiles obtained from normoxia and hypoxia. **[B]** Heatmap of significantly different metabolites ($p \leq 0.05$) between normoxia and hypoxia. Yellow - high abundance, purple - low abundance. **[C]** Significantly altered carnitine metabolites between normoxia and hypoxia. **[D]** Schematic of mitochondrial carnitine shuttling. **[E]** Glycolytic intermediates identified as significantly altered. Arrow showing the direction of the glycolytic pathway. Data generated from 4 separate monocyte preparations. Statistically analysed by Mann-Whitney test. Line shows the Mean. * $p \leq 0.05$.

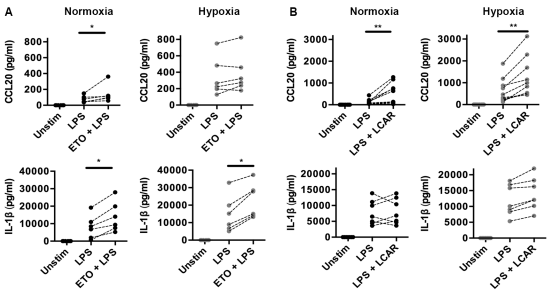

Figure 3. Carnitine modulation implicates a role for FAO in the production of pro-inflammatory mediators. [A] Monocytes were pre-treated with ETO (50 μM) for 1h and cultured for 16h in normoxia (20% O_2) or hypoxia (1% O_2) ± LPS (10 ng/ml). Supernatant was analysed by ELISA. Data statistically analysed by Wilcoxon rank test. $N = 6$. **[B]** Monocytes cultured for 16h in normoxia or hypoxia ± LPS ± L-carnitine supplementation (10 mM; LCAR). Supernatant was assessed by ELISA. Data statistically analysed by Wilcoxon rank test. $N = 7$ (separate donor cohort to **[A]**). Dots are indicative of separate donors. * $p \leq 0.05$, ** $p \leq 0.01$.

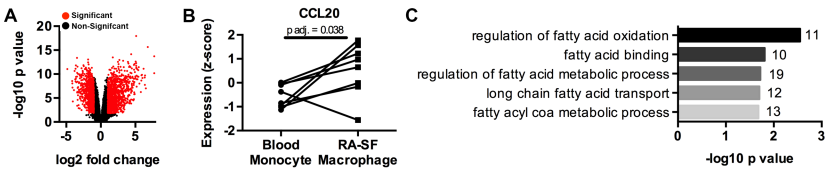

Figure 4. Monocytes transcriptionally alter CCL20 and fatty acid metabolic pathways when they infiltrate the RA synovial environment. [A-C] Microarray gene expression profile of circulating monocytes and RA-SF macrophages. **[A]** Volcano plot of circulating monocytes vs RA-SF macrophages. Significant genes (adjusted $p < 0.05$, 2-fold cut off) are shown in red and non−significant genes in black. A positive fold change indicates higher expression in macrophages than in monocytes. **[B]** Gene expression levels of CCL20 illustrated as a Z-score (distance from the mean in units of standard deviations). **[C]** Fatty acid-associated pathways identified as being significantly different in RA-SF macrophages after hypergeometric pathway analysis. Number of altered genes identified in each pathway indicated. $N = 8$. * $p \leq 0.05$.

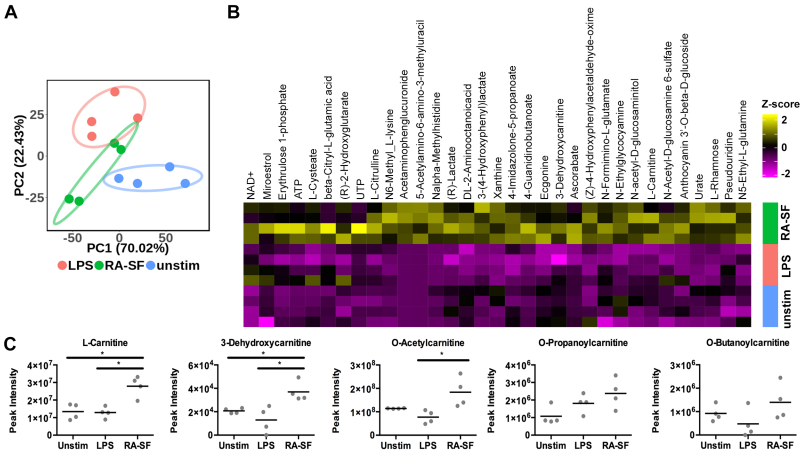

Figure 5. RA-SF increases the abundance of carnitine metabolites in human monocytes. **[A-C]** Monocytes were exposed to hypoxia for 4h and left either unstimulated or stimulated with LPS (10 ng/ml) or RA-SF (10%). The intracellular metabolites were harvested and analysed by LC-MS. **[A]** PCA analysis of the metabolic profiles of monocytes under each condition. **[B]** Heatmap of significantly increased metabolites in RA-SF treated monocytes in comparison to both unstimulated (unstim) and LPS stimulated monocytes ($p < 0.05$; Mann Whitney test). Yellow indicates high abundance and purple indicates low abundance. $N = 4$. **[C]** Carnitines and acylcarnitines that were altered in RA-SF monocytes in comparison to unstimulated and LPS stimulated cells. * $p \leq 0.05$.

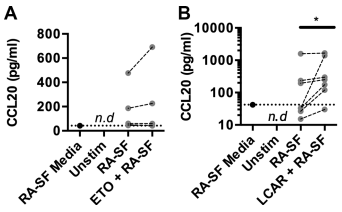

Figure 6. Exogenous carnitine increases CCL20 production in RA-SF treated monocytes in hypoxia. [A] Human monocytes were either pre-treated for 1h with ETO (50 μM) or **[B]** supplemented with L-carnitine (10 mM; LCAR) and left unstimulated or stimulated with RA-SF (10% in media). The cells were cultured for 16h in hypoxia (1% O_2) and the supernatants harvested and analysed by CCL20 ELISA. The levels of CCL20 in the RA-SF media was analysed to give baseline levels of each (dotted line). Dots are indicative of separate healthy donors of monocytes with line showing the Median. N = 5-7. Statistically analysed by Wilcoxon rank test. * $p < 0.05$. *n.d.* = non-detectable.

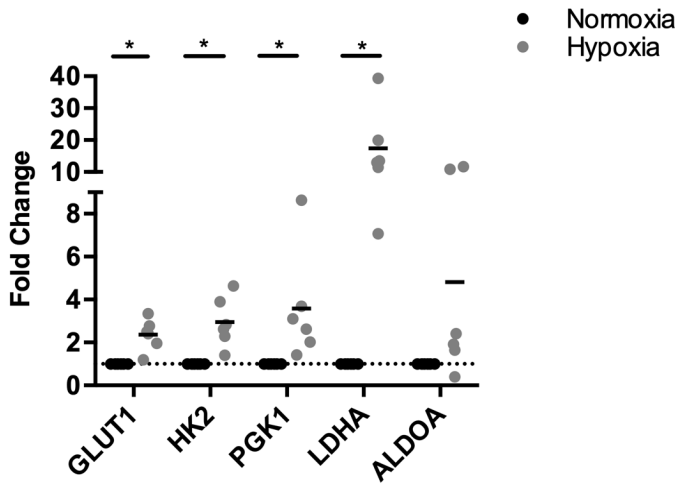

Supplementary Figure 1. Monocytes increase glycolytic gene expression under hypoxia. Monocytes were cultured in normoxia or hypoxia for 4 hours and the expression of genes of the glycolytic pathway were assessed by qPCR. Line shows the Mean. Statistically analysed by Wilcoxon Rank Test. $N = 6$. * $p \leq 0.05$.

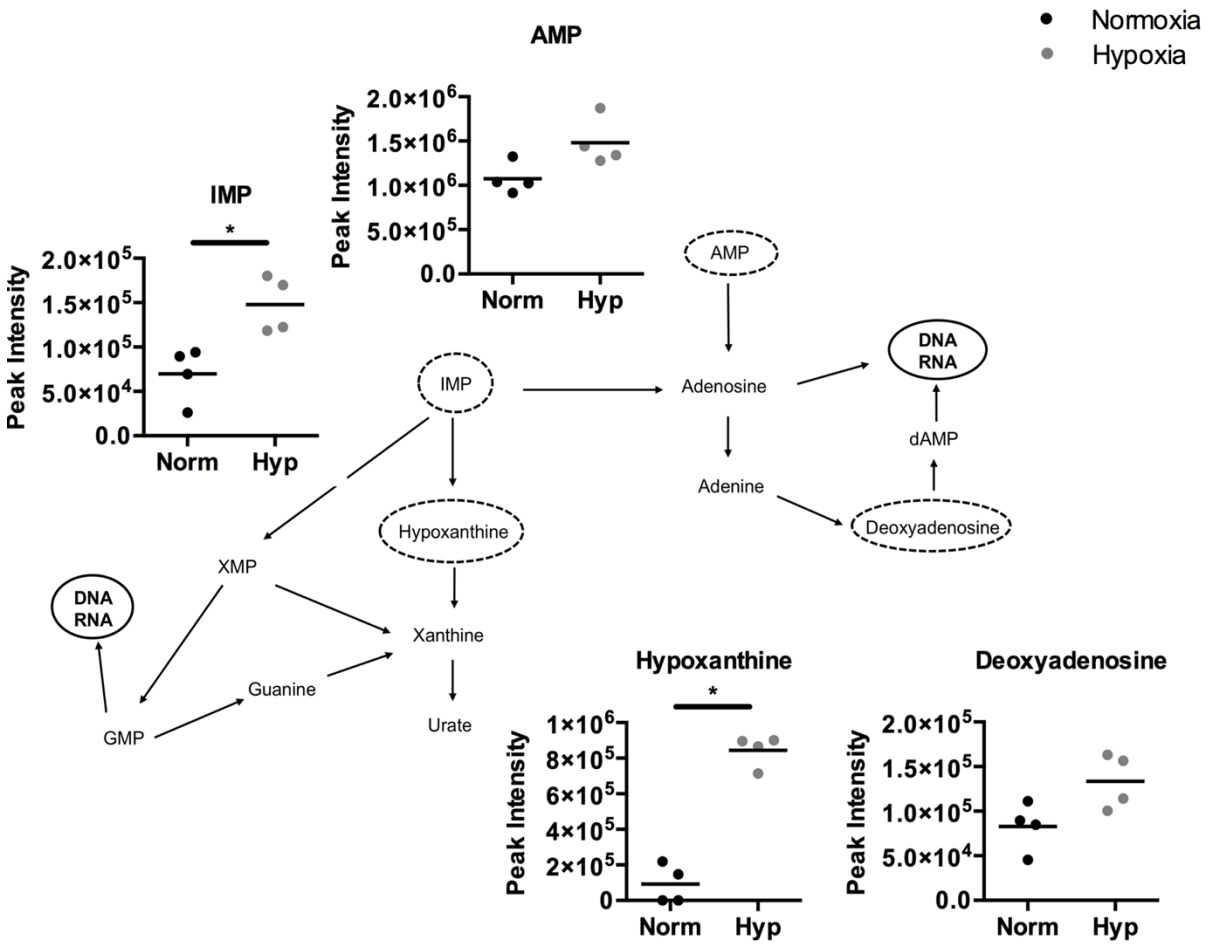

Supplementary Figure 2. Hypoxia increases the abundance of purine metabolites in human monocytes. Schematic showing the purine metabolic pathway for the synthesis of DNA and RNA. Metabolites in dashed circles indicate those that showed alterations between normoxia and hypoxia after 4 hours. The levels of these metabolites are shown graphically. The data was generated from 4 separate monocyte preparations. The data was statistically analysed by Mann Whitney test. Line shows the Mean. * $p \leq 0.05$.

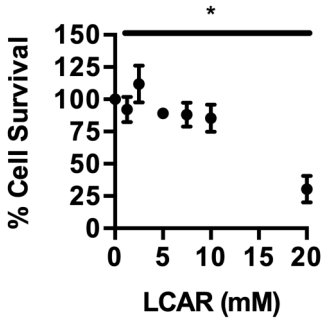

Supplemental Figure 3. High doses of carnitine negatively impact monocyte viability. Monocytes were cultured in normoxia with increasing doses of L-carnitine (LCAR; 0-20 mM) for 4 hours and toxicity was assessed by MTT assay. Dots indicative of the Mean ± SD. Statistically analysed by Friedman's test with Dunn's multiple comparison testing. $N = 3$.

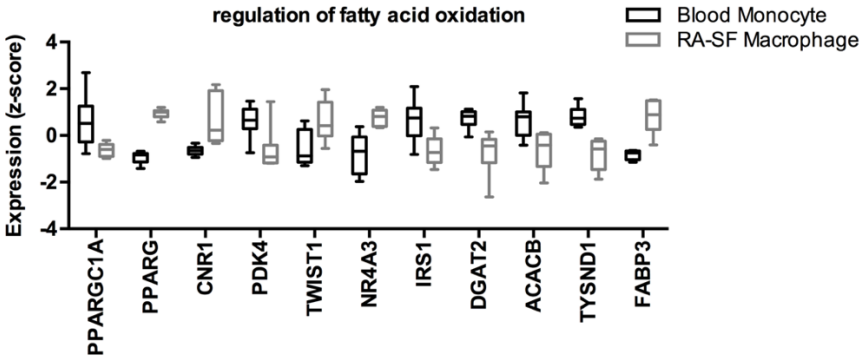
regulation of fatty acid oxidation
Blood Monocyte
RA-SF Macrophage
Expression (z-score)
4
2
0
-2
-4
PPARGC1A
PPARG
CNR1
PDK4
TWIST1
NR4A3
IRS1
DGAT2
ACACB
TYSND1
FABP3

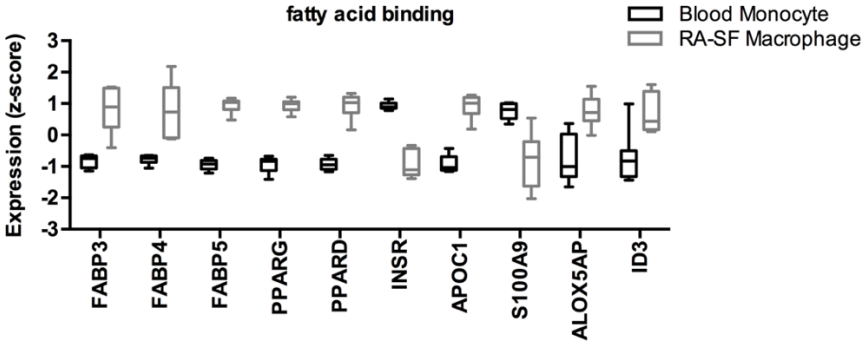
fatty acid binding
Blood Monocyte
RA-SF Macrophage
Expression (z-score)
3
2
1
0
-1
-2
-3
FABP3
FABP4
FABP5
PPARG
PPARD
INSR
APOC1
S100A9
ALOX5AP
ID3

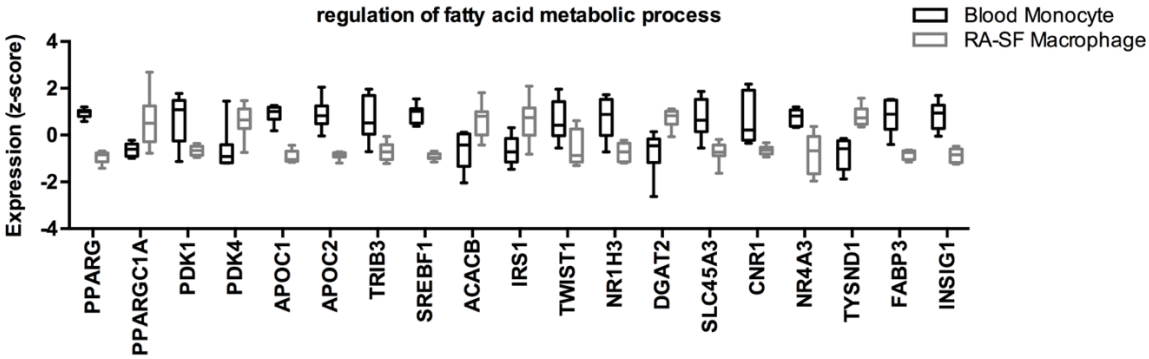
regulation of fatty acid metabolic process
Blood Monocyte
RA-SF Macrophage
Expression (z-score)
4
2
0
-2
-4
PPARG
PPARGC1A
PDK1
PDK4
APOC1
APOC2
TRIB3
SREBF1
ACACB
IRS1
TWIST1
NR1H3
DGAT2
SLC45A3
CNR1
NR4A3
TYSND1
FABP3
INSIG1

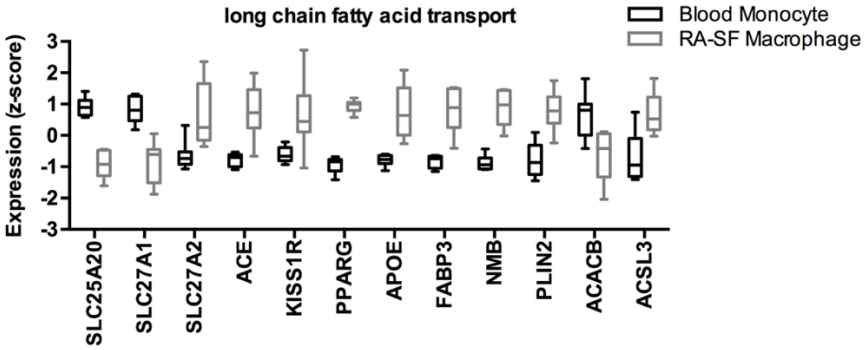
long chain fatty acid transport
Blood Monocyte
RA-SF Macrophage
Expression (z-score)
3
2
1
0
-1
-2
-3
SLC25A20
SLC27A1
SLC27A2
ACE
KISS1R
PPARG
APOE
FABP3
NMB
PLIN2
ACACB
ACSL3

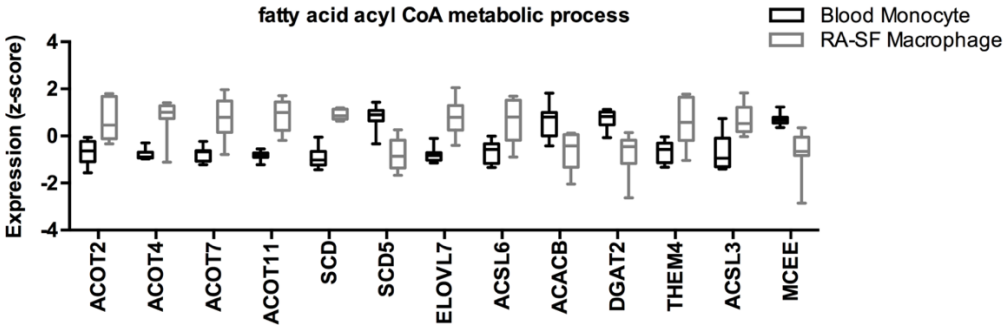
fatty acid acyl CoA metabolic process
Blood Monocyte
RA-SF Macrophage
Expression (z-score)
4
2
0
-2
-4
ACOT2
ACOT4
ACOT7
ACOT11
SCD
SCD5
ELOVL7
ACSL6
ACACB
DGAT2
THEM4
ACSL3
MCEE

Supplementary Figure 4. Pathways associated with fatty acid metabolism are altered in RA-SF macrophages in comparison to blood monocytes. Box-plots illustrating the expression levels of significantly altered genes within the fatty acid metabolic pathways identified after hypergeometric pathway analysis. *N* = 8.

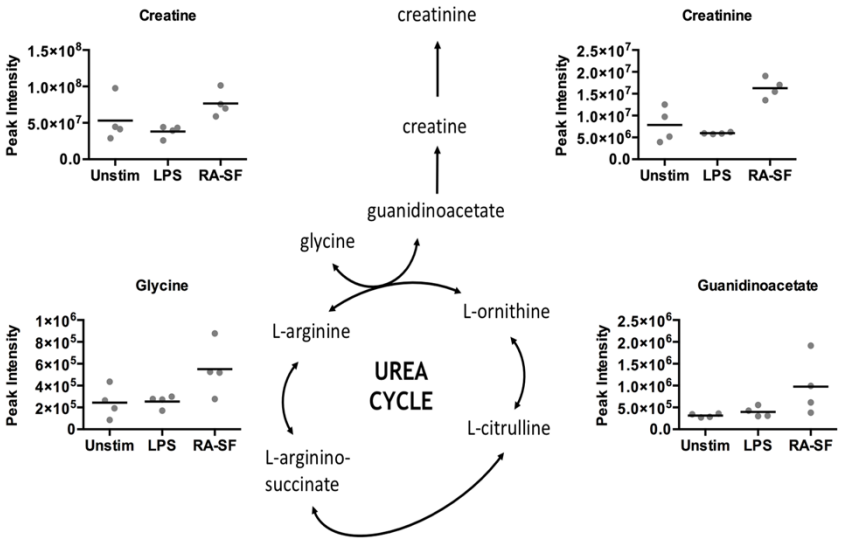

Supplementary Figure 5. Intermediates of creatinine biosynthesis are increased after stimulation with RA-SF in comparison to unstimulated and LPS stimulated monocytes. Monocytes were exposed to hypoxia for 4 hours and left either unstimulated or stimulated with LPS (10 ng/ml) or RA-SF (10%). The intracellular metabolites were harvested and analysed by LC-MS. Schematic of creatinine biosynthesis which branches off the urea cycle. Creatinine biosynthesis intermediates which were putatively identified shown graphically. Dots indicative of separate donors and line showing the Mean. *N* = 4.

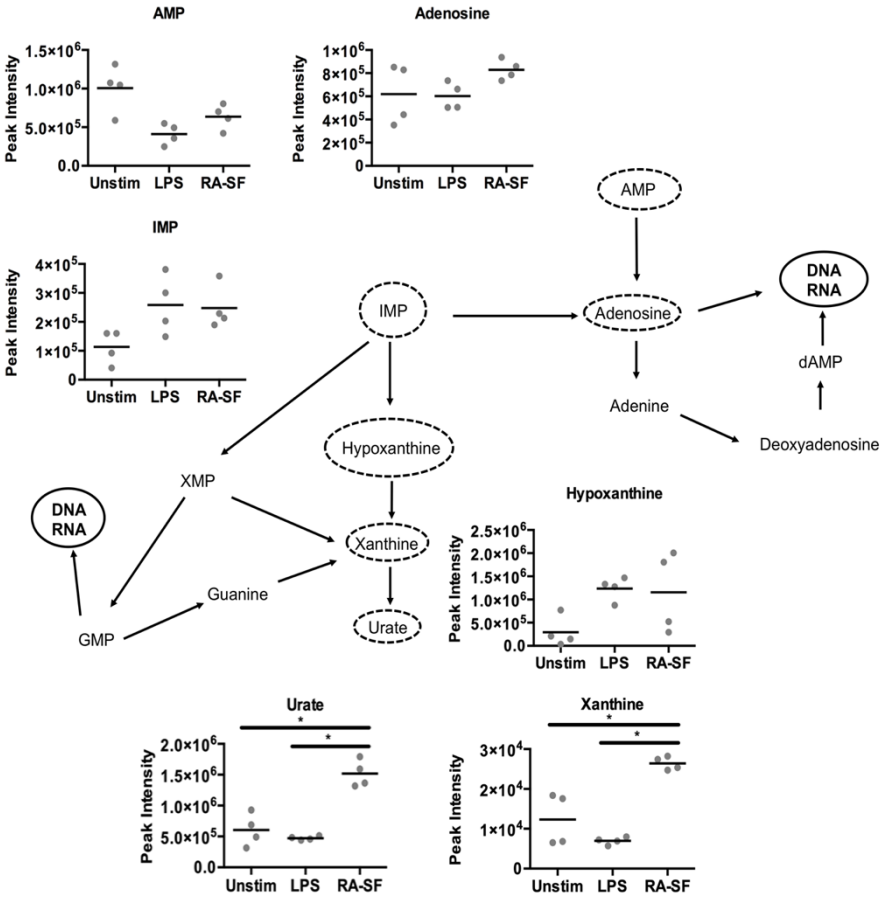

Supplementary Figure 6. Purine metabolism is altered in monocytes cultured in RA-SF in comparison to LPS and unstimulated cells. Monocytes were exposed to hypoxia for 4 hours and left either unstimulated or stimulated with LPS (10 ng/ml) or RA-SF (10%). The intracellular metabolites were harvested and analysed by LC-MS. Schematic showing the purine metabolic pathway for the synthesis of DNA and RNA. Metabolites in dashed circles indicate metabolites which were putatively identified in the dataset. The levels of these metabolites are shown graphically. Dots indicative of separate donors and line showing the Mean. Statistically analysed by Mann Whitney test. $N = 4$. * $p \leq 0.05$.

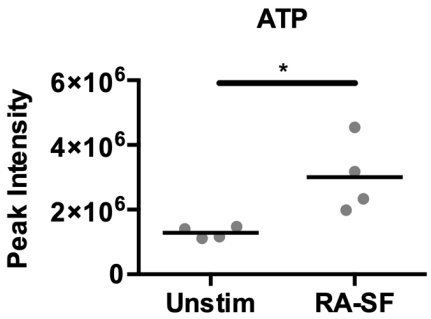

Supplementary Figure 7. ATP abundance in monocytes after LPS and RA-SF stimulation. Monocytes were cultured in hypoxia and stimulated with RA-SF for 4 hours. ATP abundance was determined via LC-MS. Dots indicative of separate donors and line showing the Mean. Statistically analysed by Mann Whitney test. $N = 4$. * $p \leq 0.05$.

Supplementary Table 1. Significantly altered metabolites in hypoxic conditions in comparison to normoxia.

KEGG ID	Metabolite	Pathway	Standard	P value	Change
C00093	sn-Glycerol 3-phosphate	Glycerolipid Metabolism	Yes	0.0286	Up
C03017	O-Propanoylcarnitine	Fatty Acid metabolism		0.0286	Down
C00118	D-Glyceraldehyde 3-phosphate	Glycolysis / PPP		0.0286	Up
No KEGG	N-(octanoyl)-L-homoserine			0.0286	Down
C00354	D-Fructose 1_6-bisphosphate	Glycolysis		0.0286	Up
C03901	Thiomorpholine 3-carboxylate			0.0286	Down
C00197	3-Phospho-D-glycerate	Glycolysis / PPP	Yes	0.0286	Up
C00065	L-Serine	Glycine, serine, threonine metabolism	Yes	0.0286	Up
C03771	5-Guanidino-2-oxopentanoate	Arginine & proline metabolism		0.0286	Down
C03741	(S)-4-Amino-5-oxopentanoate			0.0286	Down
C00042	Succinate	Tricarboxylic acid cycle	Yes	0.0286	Down
C02504	2-Isopropylmaleate	Valine, leucine and isoleucine biosynthesis		0.0286	Down
C00130	IMP	Purine Metabolism	Yes	0.0286	Up
C00670	sn-glycero-3-Phosphocholine	Glycerophospholipid metabolism	Yes	0.0286	Up
C03248	Acetylenedicarboxylate	Pyruvate Metabolism		0.0286	Down
C03824	2-Aminomuconate semialdehyde	Tryptophan metabolism		0.0286	Down
C00327	L-Citrulline	Arginine biosynthesis	Yes	0.0286	Up
C13050	Cyclic ADP-ribose	Calcium signalling pathway		0.0286	Down
C00668	D-Glucose	Glycolysis / PPP	Yes	0.0286	Up
C00064	L-Glutamine	Amino acid & Nucleotide metabolism	Yes	0.0286	Up
C06455	Hydroxymethylphosphonate	Phosphonate metabolism		0.0286	Up
C00262	Hypoxanthine	Purine Metabolism	Yes	0.0294	Up
C00447	D-Sedoheptulose 1_7-bisphosphate	Energy metabolism		0.0294	Up

Supplementary Table S2. Putatively identified metabolites in hypoxia with or without LPS or RA synovial fluid stimulation. (see attached xls file).

Supplementary Online Methods

Primary human monocyte isolation and culture

Peripheral blood mononuclear cells (PBMCs) were separated from human blood buffy coats by density gradient centrifugation using Ficoll® Paque Plus (Sigma-Aldrich) and standard procedures. To purify the monocyte population, the EasySep monocyte enrichment kit, without CD16 depletion (StemCell Technologies), was used according to manufacturer's instructions. Enriched monocytes were re-suspended at a density of $1x10^6$/ml in monocyte medium (RPMI 1640 containing 10% human pooled plasma (BioWest), 2 mM L-glutamine, 1% pen-strep). For stimulation, human monocytes were stimulated with 10 ng/ml LPS-EK ultrapure (Invivogen). Synovial fluid aspirates were collected from patients with active disease and centrifuged at 900g for 10 minutes at 4°C to remove cells and stored at -80°C. Monocytes were cultured in media containing 10% RA-SF. For carnitine manipulation, monocytes were treated with 10 mM L-carnitine (Sigma-Aldrich) simultaneously with LPS or RA synovial fluid stimulation. Monocytes were pre-treated for 1 hour with etomoxir (ETO; Sigma-Aldrich) at 50 μM.

Induction of hypoxia

For the induction of hypoxia (1% O_2), an airtight hypoxic chamber was utilised (Billups-Rothenburg). The chamber was purged with a speciality gas mixture from British Oxygen Company (BOC), containing 1% O_2, 5% CO_2 and N_2 balance, through an inlet port at a flow rate of 40 L per minute, for 3 minutes. The inlet and outlet port were sealed closed and the chamber was placed in a standard 37°C tissue culture incubator. For culture in normoxia, cells were cultured in ambient oxygen in a standard 37°C tissue culture incubator.

Immunoblotting

$1x10^6$ monocytes were lysed directly in Laemmli buffer (BioRad), boiled and loaded into NuPAGE pre-cast 4-12% Bis-Tris Gel (Thermo Fisher). Gels were transferred to PVDF

membranes and subsequently blocked with PBS-T containing 5% non-fat dried milk and incubated with antibodies specific for mouse anti-human HIF-1α (BD Transduction Laboratories) and GAPDH XP® (CST). Membranes were washed and incubated with HRP-labelled secondary antibody (Dako). After subsequent washing, membranes were incubated in WestPico substrate solution (Thermo Fisher) and visualised using an Azure Biosystems c500 Western Blot imaging system.

Extraction of monocyte intracellular metabolites

In order to quench cellular metabolism rapidly and maintain this, all reagents, vessels and procedures were performed at ≤4°C. Tissue culture plates containing monocytes were immediately placed on ice, and monocytes were aspirated and transferred to 15 ml centrifuge tubes containing ice-cold DPBS. Each well was flushed with ice-cold DPBS to remove all cells, and the flush was combined with the initial aspirated sample. Samples were centrifuged at 300g for 5 minutes at 4°C. Pellets were re-suspended in 1ml ice-cold PBS and centrifuged at 4°C. Pellets were re-suspended in 200 µl ice-cold extraction solvent (chloroform:methanol: water at a 1:3:1 ratio). The tubes were incubated for 1 hour at 4°C in an Eppendorf ThermoMixer® with shaking at 1500 rpm. Samples were centrifuged at 17,000g for 10 minutes at 4°C. Supernatant containing metabolites were collected into screw-capped vials and stored at -80°C until analysis. A pooled sample containing an equal volume of all samples (to a total of 200 µl) was generated. This sample was run during mass spectrometry analysis to assess the reproducibility of the mass spectrometer.

Untargeted Liquid Chromatography Mass Spectrometry (LC-MS)

Hydrophilic interaction liquid chromatography (HILIC) was carried out on a Dionex UltiMate 3000 RSLC system (Thermo Fisher) using a ZIC-pHILIC column (150 mm × 4.6 mm, 5 µm column, Merck Sequant). For the MS analysis, a Thermo Orbitrap Q Exactive (Thermo Fisher) was operated in both positive and negative mode. The column was

maintained at 30°C. The samples were eluted with a linear gradient from 80% acetonitrile to 20% ammonium carbonate (20 mM in water) over 24 minutes, at a flow rate of 0.3 ml/min. Each sample was run in a random order, with a pooled sample run between every 5 samples to assess for reproducibility. The MS settings were as follows: 70,000 resolution; m/z range of 70-1050; automatic gain control target of 1e6; sheath gas flow rate of 40; auxillary gas flow rate 5; sweep gas flow rate 1; probe temperature of 150°C and capillary temperature of 320°C. For positive mode ionisation: source voltage +3.8 kV, S-Lens RF Level 30.00, S-Lens Voltage -25.00 (V), Skimmer Voltage -15.00 (V), Inject Flatopole Offset -8.00 (V), Bent Flatapole DC -6.00 (V). For negative mode ionisation: source voltage-3.8 kV. The calibration mass range was extended to cover small metabolites by inclusion of low-mass calibrants with the standard Thermo calmix masses (below m/z 138), butylamine ($C_4H_{11}N_1$) for positive ion electrospray ionisation (PIESI) mode (m/z 74.096426) and COF3 for negative ion electospray ionisation (NIESI) mode (m/z 84.9906726).

Processing of MS data

Processing of the raw data and analysis was performed using a processing pipeline through IDEOM Excel based software (17). According to the metabolomics standards initiative (MSI), metabolite identifications (MSI level 1) are given when more than one feature matches an authentic standard (i.e. mass and retention time) and annotations are made when matching to a metabolite is made by mass only (MSI level 2), and should be considered putative. Included in the MS analysis was a mixture of 240 standards. These covered a range of metabolic pathways to allow metabolite identifications to be made. In the comparisons tab of the IDEOM Excel spreadsheet, the peaks were visually interrogated. Peaks not showing a Gaussian-type shape were rejected as a false identification. Due to higher than expected variation in the per sample total intensities of the LPS/SF experiment, the metabolomic data was normalised by sample total intensity. To allow for reasonable numbers the per sample

total intensity across all metabolites was set to 1,000,000. The normalised data was used in generating the principal component analysis (PCA) and heatmaps. PCA was performed on the processed metabolite data using the R (v.3.4.4) function prcomp. Ellipses were drawn around sample groups using the R function ellipse, centring on the mean x and y coordinates and scaled to 1.5 times the standard deviation. Heatmaps of significant metabolites were hierarchically clustered using the R package hclust, with the distance method Spearman and cluster method Average. The data was then scaled into per metabolite z-scores (i.e. distance from the mean in units of standard deviations) using the R function scale.

Microarray Analysis

RNA purification and microarray analysis of samples from matched RA blood and SF derived CD14+ cells was conducted as previously described (18). In brief, Raw .CEL files were processed and normalised using the R (v3.4.4). Array quality was assessed before and after normalisation. The R WGCNA package was used to collapse multiple genes down to a single value using the "MaxMean" method. This reduced the number of features from 54,675 to 21,336 unique features. Differential expression was determined using the R package LIMMA (19) with a significance threshold of adjusted $p < 0.05$ and a fold change > 2. Enriched gene-sets were determined using a hypergeometric test with Benjamini-Hochberg correction at $p < 0.05$. The collapsed probe-set was used as the background, and a combination of the following MsigDB (20) collections were used in the analysis: canonical pathways, BIOCARTA, KEGG, REACTOME and GO.

ELISA & Meso-Scale Discovery (MSD)

Supernatant analysis of IL-1β (Life Technologies) and CCL20 (R&D Systems) was carried out by ELISA according to the manufacturer's instructions. The plates were read using a Tecan Sunrise microplate reader at 450 nm (650 nm reference). The data was exported to

Excel and a standard curve was generated. The concentrations of the samples were calculated using the equation of the straight line.

TNFα, IL-1β and IL-6 supernatant were also analysed by using the V-PLEX Pro-inflammatory panel 1 from MSD according to the manufacturer's protocol. The plates were read on a MESO Quickplex SQ 120 (MSD) and the electro-chemiluminescent signal determined by using Discovery Workbench 4.0 (MSD) software.

Statistical Analysis

Statistical analysis was performed in GraphPad Prism 6 software. All data are shown as the mean ± standard deviation (SD) unless otherwise stated. The statistical test used for each experiment is indicated in the figure legend. A *p* value of less than 0.05 was considered significant.

Data Availability

The microarray array data is MIAME compliant and has been deposited to the ArrayExpress database (http://www.ebi.ac.uk/arrayexpress) with the accession number: E-MEXP-3890. Metabolomic data will be deposited to the MetaboLights database (https://www.ebi.ac.uk/metabolights).